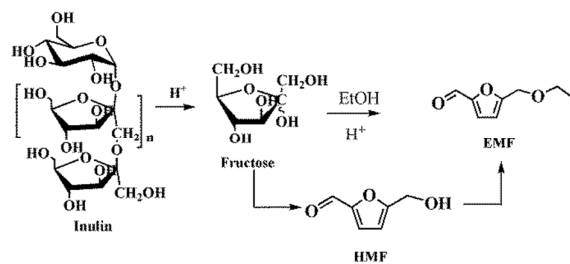




**Magnetic material grafted cross-linked imidazolium based polyionic liquids: an efficient acid catalyst for the synthesis of promising liquid fuel 5-ethoxymethylfurfural from carbohydrates**

Journal:	<i>Journal of Materials Chemistry A</i>
Manuscript ID:	TA-ART-11-2014-006135.R2
Article Type:	Paper
Date Submitted by the Author:	07-Jan-2015
Complete List of Authors:	<p>Yin, Shanshan; South-Central University for Nationalities, key Laboratory of Catalysis and Material Sciences of the State Ethnic Affairs Commission &amp; Ministry of Education</p> <p>Sun, Jie; South-Central University for Nationalities, key Laboratory of Catalysis and Material Sciences of the State Ethnic Affairs Commission &amp; Ministry of Education</p> <p>Liu, Bing; South-Central University for Nationalities, key Laboratory of Catalysis and Material Sciences of the State Ethnic Affairs Commission &amp; Ministry of Education</p> <p>Zhang, Zehui; South-Central University for Nationalities, key Laboratory of Catalysis and Material Sciences of the State Ethnic Affairs Commission &amp; Ministry of Education</p>

Magnetic material grafted polyionic liquid showed high catalytic activity for the synthesis of promising liquid fuel 5-ethoxymethylfurfural from carbohydrates



Cite this: DOI: 10.1039/c0xx00000x

www.rsc.org/xxxxxx

## Magnetic material grafted cross-linked imidazolium based polyionic liquids: an efficient acid catalyst for the synthesis of promising liquid fuel 5-ethoxymethylfurfural from carbohydrates

Shanshan Yin, Jie Sun\*, Bing Liu, Zehui Zhang\*

Received (in XXX, XXX) Xth XXXXXXXXX 20XX, Accepted Xth XXXXXXXXX 20XX

DOI: 10.1039/b000000x

Acid polyionic liquids grafted on magnetic material was successfully prepared by the radical oligomerization of bis-vinylimidazolium salts on the surface of mercaptopropyl-modified silica coated  $\text{Fe}_3\text{O}_4$ , and well characterized by several model technologies. The as-prepared magnetic catalyst ( $\text{Fe}_3\text{O}_4@\text{SiO}_2\text{-SH-Im-HSO}_4$ ) showed high catalytic activity for the synthesis of 5-ethoxymethylfurfural (EMF) from 5-hydroxymethylfurfural (HMF) and fructose based carbohydrates. The reaction temperature showed a remarkable effect on EMF yield. High EMF yield of 89.6% was obtained at 100 °C by the etherification of HMF. The one-pot conversion of fructose, sucrose and inulin catalyzed by  $\text{Fe}_3\text{O}_4@\text{SiO}_2\text{-SH-Im-HSO}_4$  generated EMF with yields of 60.4%, 34.4% and 56.1%, respectively. The catalyst could be readily separated from the reaction mixture by a permanent magnet, and showed high stability in the recycling experiments. This study shows a green and sustainable method for the synthesis of value added liquid fuel from renewable resources.

### 1. Introduction

It is well known that acid-catalyzed chemical reactions played a key role in chemical industry. Traditional acids such as HCl,  $\text{H}_2\text{SO}_4$  and  $\text{H}_3\text{PO}_4$  have been extensively used to catalyze many kinds of chemical reactions including etherification reaction, esterification reaction, hydrolysis reaction, and so forth. However, the use of homogeneous catalysts is the difficulty in separating the catalyst from the reaction mixture and the catalyst recycle. To solve the catalyst separation and recyclability problems, a promising route is the heterogenizing of homogenous catalysts,

which offers great advantages including the ease of operation conditions, reduced equipment corrosion and minimized contamination of waste streams.<sup>1,2</sup>

Ionic liquids (ILs) have received a lot of attention due to their unique properties. They are safe, nonflammable and have negligible vapor pressure with various polarities.<sup>3,4</sup> Moreover, they are tunable and can be tailored by various functionalizations and modifications. Recently, the use of ILs have attracted more attention in catalyst area, but the recyclability of expensive ILs is difficult due to their homogenous phase, which limits their widespread use in organic transformations. To overcome the recyclability problems, supported ILs catalysts have emerged extensively from the viewpoints of green and sustainable chemistry.<sup>5,6</sup> The concept of supported ILs combines the advantages of ILs with various inorganic supports such as silica particles. Although recycle of supported ILs have been largely improved as compared with the supported ILs, the tedious recovery procedure *via* filtration or centrifugation and the inevitable loss of solid catalysts in the separation process still limited the practical application of supported ILs. Nowadays, functionalized magnetic catalysts have emerged as viable alternatives to conventional heterogeneous catalysts,<sup>7,8</sup> as they offer an added advantage of being magnetically separable, thereby eliminating the requirement of catalyst filtration.

S. S. Yin Zhang, Prof. J. Sun, Dr. B. Liu and Prof. Z. H. Zhang  
Department of Chemistry, Key Laboratory of Catalysis and Material  
Sciences of the State Ethnic Affairs Commission & Ministry of  
Education.

South-Central University for Nationalities  
MinYuan Road 708, Wuhan, R.P. China  
Fax: (+)86-27-67842752

E-mail: jetsun@mail.scuec.edu.cn & zehuizh@mail.usc.edu.cn

On the other hand, under the background of green and sustainable chemistry, there is an intense search for liquid fuels and chemicals from renewable resources.<sup>9, 10</sup> Biomass as an abundant, inexpensive and CO<sub>2</sub>-neutral source of carbon, has been considered one of the most promising renewable sources. Carbohydrates as the major constitute of biomass can be dehydrated into an important furan compound 5-hydroxymethylfurfural (HMF).<sup>11-13</sup> HMF is considered to a versatile platform chemical, which are species that can be used as intermediates in the production of biofuels, such as transportation fuels and chemicals.<sup>14</sup>

5-Ethoxymethylfurfural (EMF), the etherification product of HMF with ethanol, is a promising second generation biofuel, which can serve as potential biodiesel additive or even substitute for diesel fuel,<sup>15-16</sup> owing to its high miscibility in diesel fuel. EMF is present as liquid with a high boiling point of 235 °C and it has a high energy density of 30.3 MJ/L, which is similar to that of diesel (33.6 MJ/L). Several methods have been reported for the synthesis of EMF either from HMF or glucose/fructose in excess ethanol with homogeneous acid catalysts or solid acid catalysts.<sup>17-20</sup> Homogeneous acid catalysts usually showed high catalytic activity for the synthesis of EMF. However, the furan ring of HMF is prone to hydrolytic cleavage under acidic conditions and, besides the desired EMF, a fair amount of ethyl levulinate (EL) is formed, as well. For example, the EME yield of 75% and EL yield of 15% were produced from the reaction of HMF with ethanol at 100 °C after 24 h by the use of H<sub>2</sub>SO<sub>4</sub> as the catalyst.<sup>21</sup> Later, some heterogeneous catalysts have been used for the synthesis of EMF. However, some of the heterogeneous catalysts have low acidity, resulting in low EMF yield, and the mass transformation is limited due to the limited surface area and narrow pore size.

Polyionic liquids (PILs) refer to a subclass of polyelectrolytes that feature an ILs species in each monomer repeating unit, connected through a polymeric backbone to form a macromolecular architecture. PILs has recently received a lot of attention in catalyst preparation for many chemical reactions.<sup>22, 23</sup> Some of the unique properties of ILs are incorporated into the polymer chains, giving rise to a new class of polymeric materials. In addition, PILs is facile for the reactant transfer from the reaction solution to the catalyst sites and the product release from the catalyst to the reaction solution. The acidic ionic liquids has been used for the synthesis of EMF from renewable carbohydrates,<sup>24, 25</sup> however, it seemed that the recycling of the catalyst is difficult. In this study, we described a new kind of magnetic material supported PILs with high acidity by a highly cross-linked imidazolium network obtained by radical oligomerization of bis-vinylimidazolium salts on the surface of mercaptopropyl-modified silica coated Fe<sub>3</sub>O<sub>4</sub>. This magnetic material is insensitive to air and requires no special care during its handling. With these considerations in mind, we tried to evaluate our solid acid catalyst for the synthesis of promising liquid fuel EMF from HMF and fructose based carbohydrates. To the best of our knowledge, this is the first time to report the use of magnetic material supported PILs as acid catalyst for the synthesis of EMF.

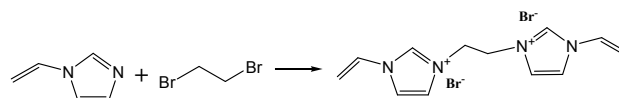
## 2. Experimental Section

### 2.1. Materials

FeSO<sub>4</sub>·7H<sub>2</sub>O (99.5 %), FeCl<sub>3</sub>·6H<sub>2</sub>O (99.5 %) 1,2-dibromoethane (99%) and tetraethoxysilane (TEOS, 99.5%) were purchased from Sinopharm Chemical Reagent Co., Ltd. (Shanghai, China). 1-Vinylimidazole (98%) and γ-mercaptopropyltrimethoxysilane (MPTMS) (98.5%) were purchased from Aladdin Chemicals Co. Ltd. (Beijing, China). Fructose was purchased from Sanland-Chem International Inc. (Xiamen, China). Inulin and sucrose were purchased from the J&K Chemical Co. Ltd., (Beijing, China). HMF (98%) was purchased by Beijing Chemicals Co. Ltd. (Beijing, China). 5-Ethoxymethylfurfural (98%) was purchased from Hangzhou Imaginechem Co., Ltd. (Zhejiang, China). Acetonitrile (HPLC grade) was purchased from Tedia Co. (Fairfield, USA). Ethanol (99.5%) was purchased from Sinopharm Chemical Reagent Co., Ltd. (Shanghai, China), and freshly distilled before use.

### 2.2 Synthesis of bis-vinylimidazolium dibromide salt

Scheme 1 illustrated the steps for the synthesis of bis-vinylimidazolium dibromide salt, and it was prepared according to known method.<sup>26</sup> A solution of 1,2-dibromoethane (0.01 mol), and 1-vinylimidazole (0.02 mol) in toluene (20 mL) was heated for 24 h in an oil bath at 90 °C with a magnetic stirring. After cooling at room temperature, the mixture was filtered and washed several times with diethyl ether to remove the unreacted starting materials including 1-vinylimidazole and dibromoethane. In order to further purify the as-prepared bis-vinylimidazolium dibromide salt, the use of active carbon was generally used to remove the colored and organic impurities with trace amount, which were not easily detected by other technologies.<sup>27</sup> The solid product was dissolved in methanol and stirred overnight in the presence of activated carbon then filtered and dried at 40 °C under reduced pressure to give rise to bis-vinylimidazolium dibromide salt in a yield of 96%. <sup>1</sup>H NMR (400 MHz, CDCl<sub>3</sub>): δ = 9.48 (s, 2H), 8.12-8.10 (d, 2H), 7.77-7.5 (d, 2H), 4.35-4.31 (t, 4H), 5.90-5.94, (t, 2H), 5.42-5.46 (d, 4H). <sup>13</sup>C NMR (100 MHz, CDCl<sub>3</sub>): 52.6, 110.6, 121.3, 124.5, 129.7, 135.8.



Scheme 1. Schematic illustration of the synthesis of bis-vinylimidazolium dibromide salt

### 2.3 Polymeric ILs supported on magnetic Fe<sub>3</sub>O<sub>4</sub>@SiO<sub>2</sub> material

Mercaptopropyl-modified silica coated Fe<sub>3</sub>O<sub>4</sub> was prepared and characterized according to our previous work.<sup>28</sup> In a round-bottom flask, 500 mg of Fe<sub>3</sub>O<sub>4</sub>@SiO<sub>2</sub>-SH was added into 20 mL of methanol, and sonicated for 30 min to homogeneously disperse in methanol. Then, bisvinylimidazolium dibromide salt (673 mg), and azobisisobutyronitrile (16.3 mg) were added into the above mixture. The whole reaction system was degassed by bubbling argon for 15 min. The mixture was heated at 78 °C under argon atmosphere with a stirring for 24 h. After reaction, the reaction mixture was cooled at room temperature, filtered under reduced

pressure and washed with hot methanol, then with diethyl ether. The obtained material was dried in an oven at 40 °C overnight.

In order to prepared acidic magnetic catalyst, the bromide ions were exchanged with hydrosulfate ions. Into the three-necked round bottom flask equipped with stirrer, the above obtained material (0.4 mg) was suspended in 3 cm<sup>3</sup> of water. During vigorous stirring, 0.15 g of concentrated H<sub>2</sub>SO<sub>4</sub> (98%) was introduced drop by drop at 0 °C. Then the mixture was warm up to the room temperature, and was refluxed for 24 h. Then water and the formed HBr were removed under reduced pressure. The excrescent H<sub>2</sub>SO<sub>4</sub> was continued washed by water until no H<sub>2</sub>SO<sub>4</sub> was remained in the solid catalyst, which was abbreviated as Fe<sub>3</sub>O<sub>4</sub>@SiO<sub>2</sub>-SH-Im-HSO<sub>4</sub> in the following.

### 2.3 Catalyst Characterization

Transmission electron microscope (TEM) images were obtained using an FEI Tecnai G<sup>2</sup>-20 instrument. The sample powder were firstly dispersed in ethanol and dropped onto copper grids for observation. X-ray powder diffraction (XRD) patterns of samples were determined with a Bruker advanced D8 powder diffractometer (Cu K $\alpha$ ). All XRD patterns were collected in the 2 $\theta$  range of 10–80° with a scanning rate of 0.016°/s. X-ray photoelectron spectroscopy (XPS) was conducted on a Thermo VG scientific ESCA MultiLab-2000 spectrometer with a monochromatized Al K $\alpha$  source (1486.6 eV) at constant analyzer pass energy of 25 eV. The binding energy was estimated to be accurate within 0.2 eV. All binding energies (BEs) were corrected referencing to the C1s (284.6 eV) peak of the contamination carbon as an internal standard. FT-IR measurements were recorded on a Nicolet NEXUS-6700 FTIR spectrometer with a spectral resolution of 4 cm<sup>-1</sup> in the wave number range of 500-4000 cm<sup>-1</sup>. The BET surface area was determined by a multipoint BET method using the adsorption data in the relative pressure ( $P/P_0$ ) range of 0.05–0.3. The mesoporous pore size distributions were derived from desorption branches of isotherms by using BJH model.

### 2.4 Titration of the acidity of the catalyst

The amount of H<sup>+</sup> in the Fe<sub>3</sub>O<sub>4</sub>@SiO<sub>2</sub>-SH-Im-HSO<sub>4</sub> was by titration with standardized aq. NaOH solution using phenolphthalein as the indicator. The Fe<sub>3</sub>O<sub>4</sub>@SiO<sub>2</sub>-SH-Im-HSO<sub>4</sub> was present in a solid state, which was not dissolved in water. Unlike the determination of acidity of the common ionic liquids, which dissolve in water, the Fe<sub>3</sub>O<sub>4</sub>@SiO<sub>2</sub>-SH-Im-HSO<sub>4</sub> (0.05 g) was firstly stirred in saturated NaCl solution (10 mL) for 24 h. The aim of this step was to use to release the HSO<sub>4</sub><sup>-</sup> part in Fe<sub>3</sub>O<sub>4</sub>@SiO<sub>2</sub>-SH-Im-HSO<sub>4</sub> to the solution to facilitate the titration (the neutralization of HSO<sub>4</sub><sup>-</sup> with NaOH). Then, the mixture was titrated with 0.01 M standard NaOH solution. The titration was stopped when the color of the solution was immediately changed from colourless to light red. The amount of H<sub>3</sub>O<sup>+</sup> in HSO<sub>4</sub><sup>-</sup> was equal to the amount of the consumed NaOH.

### 2.5 Typical procedure for the synthesis of EMF

Typically, a 10 mL stainless steel vessel with a Teflon lining was charged with HMF (126 mg, 1 mmol), Fe<sub>3</sub>O<sub>4</sub>@SiO<sub>2</sub>-SH-Im-HSO<sub>4</sub> (100 mg) and ethanol (5 mL). The reaction was carried out

at 100 °C with a magnetic stirring at 600 revolutions per minute (rpm). Time zero was recorded when the reactor was immersed into the preheated oil bath. After reaction, the reactor was cooled down to room temperature, and the reaction solution was analyzed by High-performance liquid chromatography (HPLC).

When using fructose based carbohydrates as the starting material, 1 mmol of hexose unit was used, and otherwise steps were worked up in a manner similar to that discussed above.

As one molecule HMF or hexose unit gave one molecule EMF, conversion and EMF yield were calculated according to the following equations.

$$\text{HMF conversion} = \text{moles of HMF} / \text{moles of starting HMF} \times 100\%$$

$$\text{EMF yield} = \text{moles of EMF} / \text{moles of starting HMF} \times 100\%$$

When using fructose as starting material, products yields and fructose conversion are defined as follows:

$$\text{EMF yield} = \text{moles of EMF} / \text{moles of starting fructose} \times 100\%$$

$$\text{Fructose conversion} = \text{moles of fructose} / \text{moles of starting fructose} \times 100\%$$

### 2.6 Determination of the Products

The amount of HMF and EMF in the reaction solution was analyzed by a ProStar 210 HPLC system. The typical HPLC chromatogram of EMF and HMF is shown in Fig. 1. EMF and HMF were well separated by a reversed-phase C18 column (200×4.6 mm), and they were sensitive to a UV detector at a wavelength of 280 nm. 0.1 wt.% acetic acid aqueous solution and acetonitrile at a volume ratio of 7:3 were used as the mobile eluent, and the flow rate was 0.6 mL min<sup>-1</sup>. The column temperature was maintained at 30 °C. As shown in Fig. 1, EMF and HMF were well separated under the analytic conditions, and their retention time was 3.0 and 4.0 min, respectively. The amounts of HMF and EMF were calculated based on external standard curves constructed with authentic samples.

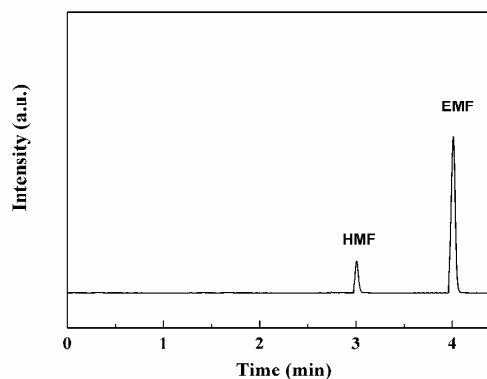


Fig. 1. The typical HPLC chromatogram of EMF and HMF.

Sugars were separated with an aminex column HPX-87 column and Refractive Index detector. 5 mM H<sub>2</sub>SO<sub>4</sub> aqueous solution was used as the mobile phase at a rate of 0.6 ml min<sup>-1</sup>.

The by-products such as ethyl levulinate was analyzed by gas chromatography (GC) on a 7890F instrument with a crosslinked capillary FFAP column (30 m × 0.32 mm × 0.4 mm) equipped with a flame ionization detector. Operating conditions were as follows: The flow rate of the N<sub>2</sub> carrier gas was 40 mL/min, the injection port temperature was 250 °C, the oven temperature was

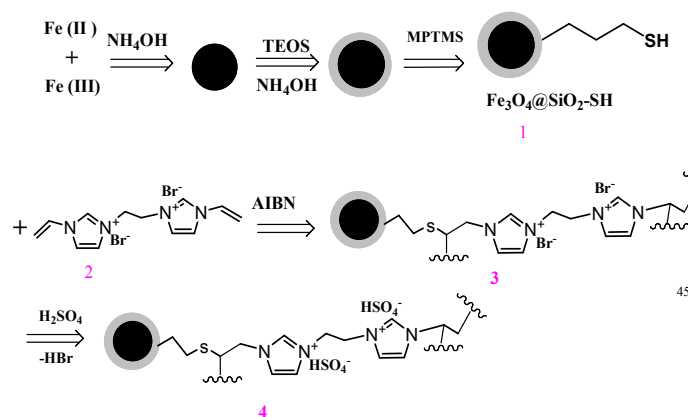
190 °C, and the detector temperature was 280 °C. The peak of ethyl levulinate was identified by comparison of standard compound and quantified based on the internal standard method.

### 2.7 Recycling of Catalyst

5 After reaction, the  $\text{Fe}_3\text{O}_4@\text{SiO}_2\text{-SH-Im-HSO}_4$  catalyst was collected with the aid of an external magnet, washed three times with ethanol, and dried at 60 °C overnight in a vacuum oven. The spent catalyst was reused for the next cycle under the same reaction conditions.

## 10 3. Results and Discussion

### 3.1 Synthesis and Characterization of the catalyst



**Scheme 2.** Scheme of the procedure of the synthesis of magnetic  $\text{Fe}_3\text{O}_4@\text{SiO}_2\text{-SH-Im-HSO}_4$  acid catalyst.

As shown in Scheme 2, the procedure of the synthesis of  $\text{Fe}_3\text{O}_4@\text{SiO}_2\text{-SH-Im-HSO}_4$  included several steps.  $\text{Fe}_3\text{O}_4@\text{SiO}_2\text{-SH}$  (compound 1) was prepared and characterized as described in our previous work.<sup>24</sup> Bis-vinylimidazolium dibromide salt (compound 2) was obtained by the reaction of 1,2-dibromoethane and 1-vinylimidazole. Material 3 was obtained by the click reaction between the hydrosulfuryl (-SH) in compound 1 and -enyl (C=C) in compound 2 in the presence of azobisisobutyronitrile (AIBN) in methanol under inert atmosphere. This reaction offers all the desirable features of a click reaction, being highly efficient, simple to execute with no side products and proceeding relatively rapidly to high yield. Since the bis-vinylimidazolium salt was added in excess relative to the amount of thiol groups the formation of imidazolium cross-linked networks through self-addition reaction of the double bonds was expected. The loading of imidazolium ring in the catalyst was calculated to be 2.2 mmol  $\text{g}^{-1}$  according to weight difference between material 3 and material 1. The bromide ions in the material 3 were finally exchanged with hydrosulfate ions by the reaction of material 3 with  $\text{H}_2\text{SO}_4$ , generating the magnetic acid catalyst (compound 4). The acidity of the  $\text{Fe}_3\text{O}_4@\text{SiO}_2\text{-SH-Im-HSO}_4$  was determined to be 1.4 mmol  $\text{g}^{-1}$  based on acid-base titration. According to the structure of the catalyst 4, one imidazolium ring was combined with a hydrosulfate ion.

40 However, the value of the acid amount was lower than that of imidazolium ring. These results indicated that some bromide ions were not successfully exchanged with the hydrosulfate ion.

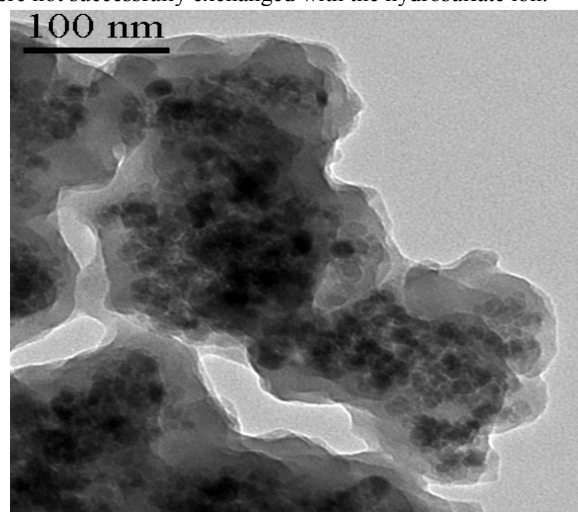


**Fig. 2.** TEM images of the  $\text{Fe}_3\text{O}_4@\text{SiO}_2\text{-SH-Im-HSO}_4$  catalyst.

45 The heterostructure of the as-prepared  $\text{Fe}_3\text{O}_4@\text{SiO}_2\text{-SH-Im-HSO}_4$  catalyst can be verified by transition electron microscopy, and the typical TEM image is shown in Fig. 2. The dark area should be the part of  $\text{Fe}_3\text{O}_4@\text{SiO}_2$ . The dark area was coated with a thick organic layer. As reported in the Scheme 2, the click reaction of the hydrosulfuryl (-SH) in compound 1 and -enyl (C=C) in compound 2 readily occurred in the presence of radical initiator (AIBN). As the amount of compound 2 was much larger than that of hydrosulfuryl (-SH), compound 2 was self connected on the surface of  $\text{Fe}_3\text{O}_4@\text{SiO}_2\text{-SH}$  by the click reaction of the -enyl (C=C) groups. Thus a thick organic layer could be observed. The TEM results clearly indicated that  $\text{Fe}_3\text{O}_4@\text{SiO}_2\text{-SH}$  was successfully grafted with poly ionic liquid layer.

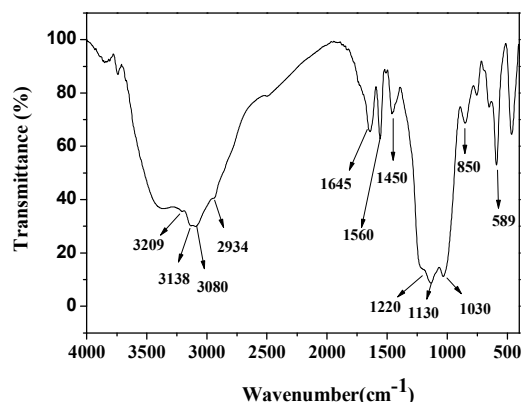


**Fig. 3** FTIR spectra of the  $\text{Fe}_3\text{O}_4@\text{SiO}_2\text{-SH-Im-HSO}_4$  catalyst.

The structure of the  $\text{Fe}_3\text{O}_4@\text{SiO}_2\text{-SH-Im-HSO}_4$  catalyst was further characterized by FT-IR technology and the results are shown in Fig. 3. A strong peak at  $589\text{ cm}^{-1}$  is the characteristic Fe–O vibration of  $\text{Fe}_3\text{O}_4$ , suggesting that  $\text{Fe}_3\text{O}_4$  is present in the catalyst.<sup>29</sup> The anti symmetric Si-O-Si stretching vibration was observed with the center around  $1030\text{ cm}^{-1}$ .<sup>30</sup> The presence of the  $\text{HSO}_4^-$  was also verified by the O=S=O asymmetric and symmetric stretching modes were presented in  $1220\text{ cm}^{-1}$  and  $1130\text{ cm}^{-1}$  respectively.<sup>30</sup> At the same time, the bands at  $1560$  and  $1645\text{ cm}^{-1}$  were the in-plane C=C and C=N stretching vibrations of the imidazolium ring.<sup>31</sup> The peak at  $850\text{ cm}^{-1}$  is assigned to the C-H in-plane vibration of imidazolium ring.<sup>31</sup> In addition,  $1450\text{ cm}^{-1}$  was attributed to the symmetrical deformation vibrations of alkyl chain.<sup>29</sup> The peak at  $2934\text{ cm}^{-1}$  is assigned to the symmetrical stretching vibration of alkyl chain.<sup>32</sup> Features above  $3000\text{ cm}^{-1}$  were from the C-H vibrational modes of the imidazolium ring, where peaks at  $3080$ ,  $3138$  and  $3209\text{ cm}^{-1}$  were assigned stretch vibrational modes of C(2)-H, C(4)-H, C(5)-H in the imidazolium ring.<sup>33</sup> The peak at  $3330\text{ cm}^{-1}$  was attributed to the stretching vibration of –OH in  $\text{HSO}_4^-$ .

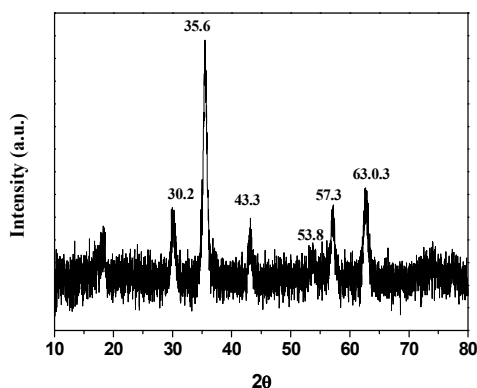


Fig. 4. XRD patterns of the  $\text{Fe}_3\text{O}_4@\text{SiO}_2\text{-SH-Im-HSO}_4$  catalyst.

As shown in Fig. 4, the X-ray diffraction (XRD) pattern of the  $\text{Fe}_3\text{O}_4@\text{SiO}_2\text{-SH-Im-HSO}_4$  shows characteristic peaks and relative intensities, which matched well with the standard  $\text{Fe}_3\text{O}_4$  sample (JCPDS file No. 19-0629).<sup>34</sup> Six characteristic diffraction peaks were observed at  $2\theta = 30.2^\circ$ ,  $35.6^\circ$ ,  $43.3^\circ$ ,  $53.8^\circ$ ,  $57.3^\circ$  and  $63.0^\circ$ , and these peaks were attributed to (220), (311), (400), (422), (511) and (440) Bragg reflections of face-centered cubic lattice of  $\text{Fe}_3\text{O}_4$  nanoparticles, respectively (JCPDS No. 19-0629). In addition, there were no diffraction peaks for the polyionic liquids layer.

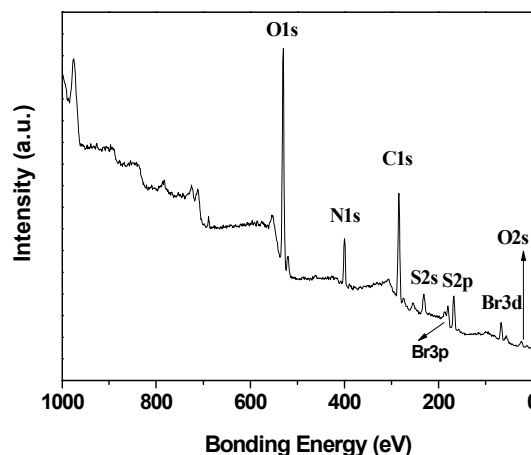
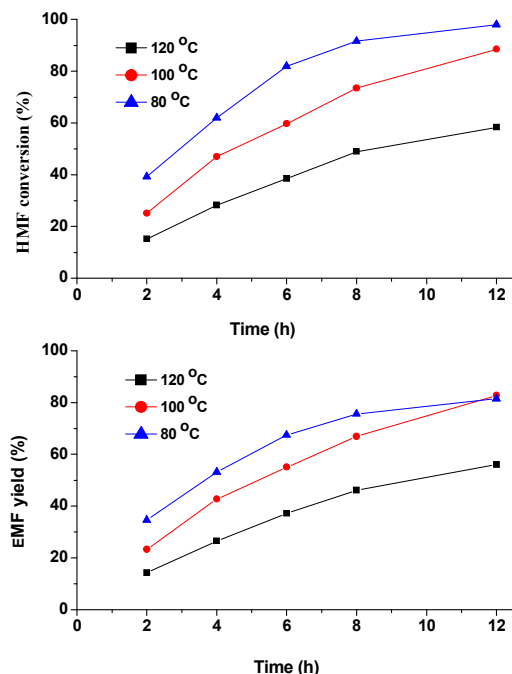


Fig. 5 XPS spectra of the  $\text{Fe}_3\text{O}_4@\text{SiO}_2\text{-SH-Im-HSO}_4$  catalyst.

The surface elementary composition and valence state of elements were characterized by XPS technology, and the results are shown in Fig. 5. These peaks with the binding energy at  $530.5$ ,  $400.2$ ,  $284.3$ ,  $231.4$ ,  $187.2$ ,  $180.2$ ,  $167.5$  and  $66.2\text{ eV}$  were assigned to O 1s, N 1s, C 1s, S 2s, Br  $3p_{1/2}$ , Br  $3p_{3/2}$ , S 2p and Br 3d, respectively. These XPS results indicated that the surface elements were composed of N, O, C, S, and Br. The presence of Br indicated that  $\text{Br}^-$  was partially exchanged with the  $\text{HSO}_4^-$  during the catalyst preparation process. These results were consistent with the results that the acidity of the catalyst was lower than the calculated acidity according to the amount of imidazole ring, which we have discussed above. The XPS results also showed that there were no silica and iron present on the surface of the catalyst, indicating that  $\text{Fe}_3\text{O}_4@\text{SiO}_2$  was encapsulated by the layer, and it was consistent with the TEM results as shown in Fig. 2, in which a thin poly ionic liquid layer was observed.

### 3.2 Effect of reaction temperature on the synthesis of EMF from HMF



**Fig. 6.** Time course of HMF conversion (a) and EMF yield (b) at different reaction temperatures. Reaction conditions: HMF (126 mg, 1 mmol),  $\text{Fe}_3\text{O}_4@\text{SiO}_2\text{-SH-Im-HSO}_4$  (100 mg), ethanol (5 mL).

The catalytic activity of  $\text{Fe}_3\text{O}_4@\text{SiO}_2\text{-SH-Im-HSO}_4$  was evaluated by the etherification of HMF into EMF with ethanol. Firstly, experiments were carried out at three different reaction temperatures from 80 to 120 °C to study the effect of reaction temperature on this reaction. As shown in Fig. 6, a significant effect of reaction temperature on HMF conversion and EMF yield is observed. It is noted that HMF conversion at three different reaction temperatures increased gradually during the time course of the reaction process. At the same reaction temperature, the higher the reaction temperature was, the higher HMF conversion was. At 80 °C, low HMF conversion of 58.3% was observed after 12 h. However, HMF conversion greatly increased to 88.5% by the increase of the reaction temperature from 80 to 100 °C. Further increasing the reaction temperature to 120 °C, almost quantitative HMF conversion (up to 98%) was achieved. These results indicated that the etherification of HMF with ethanol was sensitive to the reaction temperature.

EMF yield also increased gradually during the time course of the reaction process at three different reaction temperatures. At the same reaction time point from 2 to 8 h, EMF yield increased with the increase of the reaction temperature. For example, EMF was obtained in a low yield 14.3% within 2 h at the reaction temperature 80 °C, while it increased to be 23.3% and 34.6% within 2 h at 100 °C and 120 °C, respectively. At the end of reaction time point at 12 h, EMF yields were determined to be 56.1%, 82.7% and 81.5% for the reaction temperature of 80, 100 and 120 °C, respectively, and these corresponding selectivities

were 96.2%, 93.4% and 83.2%. It is reported that furan ring of HMF is prone to hydrolytic cleavage to give rise to ethyl levulinate at high reaction temperature.<sup>21</sup> The reaction solution was also analyzed by gas chromatography, and the yield of ethyl levulinate was determined to be 0.5%, 4.3% and 13.6% for the corresponding temperature of 80, 100 and 120 °C, respectively.

### 3.3 Effect of catalyst amount on the conversion of HMF into EMF

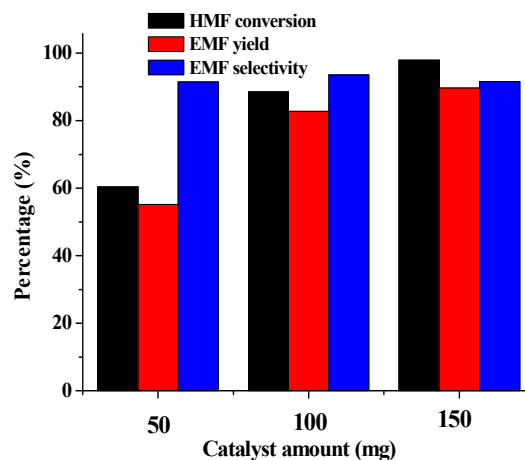


**Fig. 7.** The results of the etherification of HMF into EMF with different catalyst amounts. Reaction conditions: HMF (126 mg, 1 mmol), ethanol (5 mL), 100 °C, 12 h.

With the aim to optimal the reaction condition to obtain high HMF conversion and EMF yield, the effect of catalyst amount was studied. Fig. 7 presented HMF conversion, EMF yield and EMF selectivity. It was observed that HMF conversion and EMF yield increased with the increase of the catalyst amount. High HMF conversion of 97.9% and EMF yield of 89.6% were obtained after 12 h by the use of 150 mg of the catalyst. The increase of HMF conversion and EMF yield with an increase of the catalyst dosage should be attributed to an increase in the availability and number of catalytically active sites. However, the selectivity of EMF seemed not to be influenced by the catalyst amount, and it was almost the same around 92% with different catalyst amounts. As discussed above, the side reactions such as the formation of ethyl levulinate or humins were greatly affected by the reaction temperature, and the catalyst amount simultaneously accelerated the main reaction and the side reactions.

### 3.4 Synthesis of EMF from fructose based carbohydrates

HMF is the acid-catalyzed dehydration product of carbohydrates, especially readily from fructose, and the aforementioned etherification of HMF into EMF was also acid-catalyzed reaction. Thus it is logical to take the two isolated steps into one-pot reaction for the synthesis of EMF from fructose or other carbohydrates. The one-pot reaction for the synthesis of EMF is attractive, due to the high cost of HMF. Fructose was initially used as the substrate for the synthesis of EMF. When the reaction was carried out at 80 °C, fructose conversion was observed to be

9.5% (Table 1, Entry 1). HMF and EMF were detected as the main products with yields of 6.8% and 2.0%, respectively (Table 1, Entry 1). Therefore, in order to improve the reaction efficiency, the one-pot reaction was further carried out 100 °C. Compared with the results obtained at 80 °C, high fructose conversion of 90.4% was obtained, suggesting that the dehydration of fructose in ethanol proceeded smoothly at 100 °C. The total yield of HMF and EMF was increased from 9.5% at 80 °C to 70.1% at 100 °C (Table 1, Entry 2). Compared with the value of fructose conversion, furan yields (HMF and EMF) were lower than fructose conversion, suggesting that some side reactions occurred. Besides to the formation of EL from the alcoholysis of HMF, a small amount of brownish black humins was observed. The humins were usually produced through the self-polymerization or cross-polymerization of these intermediates, fructose, and HMF.<sup>30</sup> Although the total yield of HMF and EMF was high at 100 °C, EMF and HMF were co-present in a similar yield. This phenomenon was not the same when HMF was used as the starting material, and the reason is that the water formed from the dehydration of fructose inhibited the etherification of HMF at 100 °C. When the reaction was further carried out at 120 °C, almost quantitative fructose conversion was observed. EMF was produced as the main product in a high yield of 60.4% (Table 1, Entry 3). In addition, the yield of ethyl levulinate was determined to be 18.7%. The total yield of EMF, HMF and ethyl levulinate was lower than fructose conversion. The gap should be caused by the formation of humins during the conversion of fructose into EMF. However, it is difficult to quantify the yield of humins due to its uncertain chemical structure.<sup>34</sup>

Besides fructose, the fructose based disaccharide (sucrose) and polysaccharide (inulin) were also used as the starting materials of the synthesis of EMF. Sucrose is the most abundant and cheapest disaccharide. No sucrose was detected after 24 h at 120 °C. EMF and HMF were obtained in yield of 34.4% and 4.7%, respectively (Table 1, Entry 4). One molecule of sucrose was constituted of one glucose and one fructose unit. When glucose was subjected to this reaction, the major product was determined to be ethyl glucoside.<sup>35</sup> The results indicated that only the fructose unit in sucrose can be converted into HMF and EMF, and the acid catalyst cannot promote the isomerization of glucose to fructose. Interestingly, a good EMF yield of 56.1% was also obtained when the polysaccharides inulin was used as the substrate for the reaction (Table 1, Entry 5). These results indicated that the prepared catalyst not only catalyzed etherification and dehydration reactions, but also hydrolysis. We also analyzed the reaction solution by HPLC, and found that the reaction solution only contains fructose in a yield of 2.1%, and no other oligosaccharides were present in the reaction solution.

**Table 1** The results of the one-pot conversion of carbohydrate in ethanol.<sup>a</sup>

Entry	Substrate	Temperature (°C)	Conversion (%)	HMF yield (%)	EMF yield (%)
1	Fructose	80	9.5	6.8	2.0

2	Fructose	100	90.4	30.7	39.2
3	Fructose	120	98.4	3.5	60.4
4	Sucrose	120	100	4.7	34.4
5	Inulin	120	-	2.8	56.1

<sup>a</sup> Reaction conditions: Substrate (1 mmol of hexose unit), Fe<sub>3</sub>O<sub>4</sub>@SiO<sub>2</sub>-SH-Im-HSO<sub>4</sub> (100 mg), ethanol (5 mL), 24 h.

### 3.5 Catalyst recycling experiments

Finally, the reusability and stability of the Fe<sub>3</sub>O<sub>4</sub>@SiO<sub>2</sub>-SH-Im-HSO<sub>4</sub> catalyst was investigated, and the etherification of HMF into EMF was used as the model reaction. After the reaction, the catalyst could be readily collected by an external magnet. The spent catalyst was then washed three times with ethanol and dried at 60 °C overnight. The spent catalyst was used for the second cycle under the same reactions as described for the first cycle. These steps were repeated for six times. As shown in Fig. 8, EMF yield was almost the same around 90% in each run. More importantly, we have also determined the acidity of the spent catalyst after six runs. The acidity of the spent catalyst was determined to be 1.4 mmol g<sup>-1</sup>, which was the same with the fresh catalyst. These results clearly indicated that the catalyst could be reused without the loss of its catalytic activity.

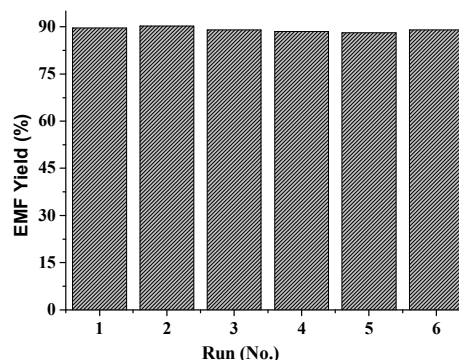


**Fig. 8** Recycle experiments of Fe<sub>3</sub>O<sub>4</sub>@SiO<sub>2</sub>-SH-Im-HSO<sub>4</sub>. Reaction condition: HMF (1 mmol, 126 mg), catalyst (150 mg), ethanol (5 mL), 12 h.

## 4. Conclusions

In summary, we have successfully prepared a magnetic material supported polyionic liquids acid catalyst and used for the synthesis of high-heating value liquid biofuel EMF from the etherification of HMF or the one-step conversion of fructose-based carbohydrates. The prepared catalyst showed an excellent catalytic activity for the etherification of HMF in ethanol with a high EMF yield of 89.6%. The one-pot conversion of fructose, sucrose and inulin catalyzed by Fe<sub>3</sub>O<sub>4</sub>@SiO<sub>2</sub>-SH-Im-HSO<sub>4</sub> generated EMF with yields of 60.4%, 34.4% and 56.1%, respectively. Finally, the Fe<sub>3</sub>O<sub>4</sub>@SiO<sub>2</sub>-SH-Im-HSO<sub>4</sub> catalyst

could be readily collected from the reaction solution by an external magnet and reused for several times without the loss of its catalytic activity. Thus, the present developed method opens a new route in green and sustainable industry for the one step conversion of abundant and cheaper fructose-based carbohydrates into the promising biofuel EMF.

### Acknowledgements

The Project was supported by National Natural Science Foundation of China (No. 21203252), and the Chenguang Youth Science and Technology Project of Wuhan City (No. 2014070404010212).

### References

- 1 P. Gupta and S. Paul, *Catal. Today* 2014, **236**, 153-170.
- 2 F. Su and Y.H. Guo, *Green Chem.* 2014, **16**, 2934-2957.
- 3 H. L. Yang, S. W. Li, X. Y. Zhang, X. Y. Wang and J. T. Ma, *J. Mater. Chem. A* 2014, **2**, 12060-12067.
- 4 T. L. Greaves and C. J. Drummond, *Chem. Soc. Rev.* 2013, **42**, 1096-1120.
- 5 T. Huang, B. Liu, Z. H. Zhang, Y. H. Zhang and J. L. Li, *RSC Adv.* 2014, **4**, 28529-28536.
- 6 M. I. Kim, S. J. Choi, D. W. Kim, D. and W. Park, *J. Ind. Eng. Chem.* 2014, **20**, 3102-3107.
- 7 H. Naeimi and S. Mohamadabadi, *Dalton Trans.* 2014, **43**, 12967-12973.
- 8 Z. H. Zhang, B. Liu, K. L. Lv, J. Sun and K.J. Deng, *Green Chem.* 2014, **16**, 2762-2770.
- 9 L. Basile, A. Tugnoli, C. Stramigioli and V. Cozzani, *Fuel* 2014, **37**, 277-284.
- 10 G. Chatel, K. D. Vigier and F. Jerome, *ChemSusChem* 2014, **7**, 2774-2787.
- 11 S. H. Xiao, B. Liu, Y. M. Wang, Z. F. Fang and Z. H. Zhang, *Bioresource Technol.* 2014, **151**, 361-366.
- 12 B. Liu, Z. H. Zhang, K. L. Lv, K. J. Deng and H. M. Duan, *Appl. Catal. A: Gen.* 2014, **472**, 64.
- 13 M. Dashtban, A. Gilbert and P. Fatehi, *RSC Adv.* 2014, **4**, 2037-2050
- 14 R. J. van Putten, J. C. van der Waal, E. de Jong, C. B. Rasrendra, H. J. Heeres and J. G. de Vries, *Chem. Rev.* 2013, **113**, 1499-597.
- 15 M. Mascal and E. B. Nikitin, *ChemSusChem* 2009, **2**, 423-426;
- 16 G. A. Kraus and T. Guney, *Green Chem.* 2012, **14**, 1593-1598.
- 17 C. M. Lew, N. Rajabbeigi and M. Tsapatsis, *Ind. Eng. Chem. Res.* 2012, **51**, 5364-5366.
- 18 B. Liu, Z. H. Zhang, K. C. Huang, and Z. F. Fang, *Fuel*, 2013, **113**, 625-631.
- 19 M. Mascal and E. B. Nikitin, *Angew. Chem. Int. Ed.* 2008, **120**, 8042-8044.
- 20 A. Q. Liu, B. Liu, Y. M. Wang, R. S Ren and Z. H. Zhang, *Fuel* 2014, **117**, 68-73.
- 21 M. Balakrishnan, E. R. Sacia and A. T. Bell, *Green Chem.* 2012, **14**, 1626-1659.
- 22 S. M. Sarkar, Y. Uozumi and Y. M. Yamada, *Angew. Chem. Int. Ed.* 2011, **50**, 9437-9441.
- 23 Q. Zhao, P. Zhang, M. Antonietti and J. Yuan, *J. Am. Chem. Soc.* 2012, **134**, 11852-11855.
- 24 S. Saravanamurugan, O. N. Van Buu and A. Riisager, *ChemSusChem* 2014, **4**, 723-726.
- 25 M. I. Alam, S. De, S. Dutta, B. Saha, *RSC Adv.* 2012, **2**, 6890-6896.
- 26 P. Agrigento, M. J. Beier, J. T. N. Knijnenburg, A. Baiker, M. Gruttadauria, *J. Mater. Chem.* 2012, **22**, 20728-20735.
- 27 A. K. Burrell, R. E. Del Sesto, S. N. Baker, T. M. McCleskey, G.A. Baker, *Green Chem.* 2007, **9**, 449-454.
- 28 Z. H. Zhang, Z. L. Yuan, D. G. Tang, Y. S. Ren, K. L. Lv and B. Liu, *ChemSusChem* 2014, **7**, 3496-3504.
- 29 S. H. Xuan, L. Y. Hao, W. Q. Jiang, X. L. Gong, Y. Hu and Z. Y. Chen, *J. Magn. Magn. Mater.* 2007, **308**, 210-213.
- 30 B. Girisuta, L. P. B. M. Janssen and H. J. Heeres, *Green Chem.* 2006, **8**, 701-709.
- 31 S. Feng and Y. Q. Deng, *Spectrochimica Acta Part A* 2005, **62**, 239-244.
- 32 E. R. Talaty, S. Raja, V. J. Storhaug, A. Doll and W. R. Carper, *J. Phys. Chem. B* 2004, **108**, 13177-13184.
- 33 D. A. Carter, J. E. Pemberton and K. J. Woelfel, *J. Phys. Chem. B* 1998, **102**, 9870-9880.
- 34 J. Wang, W. Xu, J. Ren, X. Liu, G. Lu and Y. Wang, *Green Chem.* 2011, **13**, 2678-2681.
- 35 B. Liu and Z. H. Zhang, *RSC Adv.* 2013, **3**, 12313-12319.